JACS
JOURNAL OF THE AMERICAN CHEMICAL SOCIETY

Communication

pubs.acs.org/JACS

Bottom-Up Strategy To Prepare Nanoparticles with a Single DNA Strand

Hang Xing,[†,‡,§] Yugang Bai,[†,§] Yunhao Bai,[†] Li Huey Tan,[†] Jing Tao,[†] Benjamin Pedretti,[†] Gretchen A. Vincil,[†] Yi Lu,[*,†,‡] and Steven C. Zimmerman[*,†]

[†]Department of Chemistry, University of Illinois at Urbana−Champaign, Urbana, Illinois 61801, United States

[‡]Beckman Institute for Advanced Science and Technology, University of Illinois at Urbana−Champaign, Urbana, Illinois 61801, United States

Supporting Information

ABSTRACT: We describe the preparation of cross-linked, polymeric organic nanoparticles (ONPs) with a single, covalently linked DNA strand. The structure and functionalities of the ONPs are controlled by the synthesis of their parent linear block copolymers that provide monovalency, fluorescence and narrow size distribution. The ONP can also guide the deposition of chloroaurate ions allowing gold nanoparticles (AuNPs) to be prepared using the ONPs as templates. The DNA strand on AuNPs is shown to preserve its functions.

For two decades, DNA-functionalized nanoparticles (DNA-NPs) have been intensely studied.[1] In addition to being excellent building blocks for nanoscale assembly,[2] DNA-NPs are well suited to biosensing and therapeutic applications.[3] Despite this considerable progress, a remaining challenge is in the preparation of DNA-NPs with a single DNA strand per NP. The fabrication of desired nanostructures and subsequent applications very much depends on NP valency.[4] In particular, better spatial control of NP assembly and improved sensing and imaging results would benefit from a facile preparation of monovalent DNA-NPs.[5]

Most of the strategies to prepare monovalent DNA-NPs reported to date have focused on ligand exchange methods, wherein a layer of loosely bound capping agents on the NP surface is exchanged with DNA strands bearing a functional end-group.[6] The exchange process is followed by postsynthetic purification using gel electrophoresis or anion-exchange HPLC.[7] One method to improve the yield of monovalent products uses steric hindrance or surface-based masking strategies that block part of the NP surface.[8] Another approach features bidentate or multidentate ligands that provide greater stability in the resultant monovalent DNA-NP.[9] These approaches typically involve a difficult purification, but the more traditional ligand exchange approaches have indeed enabled gold NPs (AuNP), silver NPs (AgNP) and quantum dots to be linked with a single functional DNA using metal−thiol chemistry.[5a,d,7a,9c] Because the DNA functionality is introduced after the formation of NP, a suitable surface conjugation chemistry is a must for successful monovalent DNA-NP synthesis and can be limiting in some circumstances.

In considering the challenges potentially encountered in preparing monovalent DNA-NP by the above methods, it is instructive to examine alternative methods of NP synthesis. For example, it is possible to "cast" the NPs within a template or "mold" with defined dimensions and function, such as a virus or an organic, organometallic, or DNA cage.[10] NPs have also been prepared by metal deposition within metal−organic frameworks and a wide range of polymers.[11] Templated approaches expand the generality of NP synthesis; however, controlling valency in this manifold does not seem to have been examined, possibly because the template surface is generally isotropic with multiple reactive sites that may or may not remain linked to the NP.

Herein we describe a bottom-up strategy that features a facile synthesis of monovalent DNA-functionalized polymeric organic nanoparticles (DNA-ONPs) that in turn serve as templates for the formation of monovalent metal NPs. The central idea is that a polymer-based, bottom-up approach can guide the synthesis of DNA-NP conjugates from the molecular level, allowing control of particle valence. As illustrated schematically in Figure 1, the approach relies on four key steps: (1) copolymerization of functionally reactive and inert monomers with a single reactive group at the chain-end, (2) intramolecular cross-linking of the parent linear polymer leading to single-chain collapse and formation of an ONP, (3) conjugation of a single DNA strand to each ONP, and (4) metal deposition using the DNA-ONP conjugate as a template. This approach combines the inherent ease by which polymers can be end-

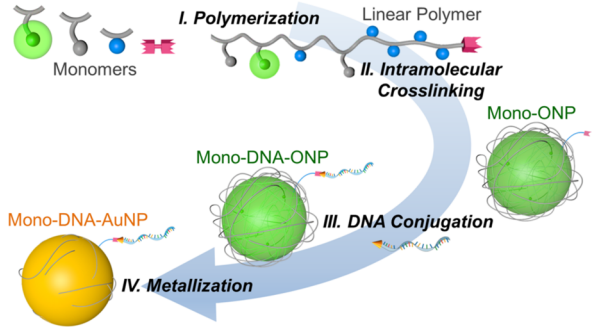

Figure 1. Schematic showing the stepwise, bottom-up synthesis of monovalent DNA-NP conjugate using single-chain block copolymer as template.

Received: January 3, 2017
Published: March 6, 2017

DOI: 10.1021/jacs.7b00065
J. Am. Chem. Soc. 2017, 139, 3623−3626

functionalized with newly developed methods for intramolecular cross-linking that produce a single chain polymeric nanoparticle (SCNP) with well-defined dimensions and suitable internal groups.

The first two steps paralleled our recently reported synthesis of monofunctional ONPs (SCNPs), with some key modifications.[12] Thus, as outlined in Figure 2, the linear polymer

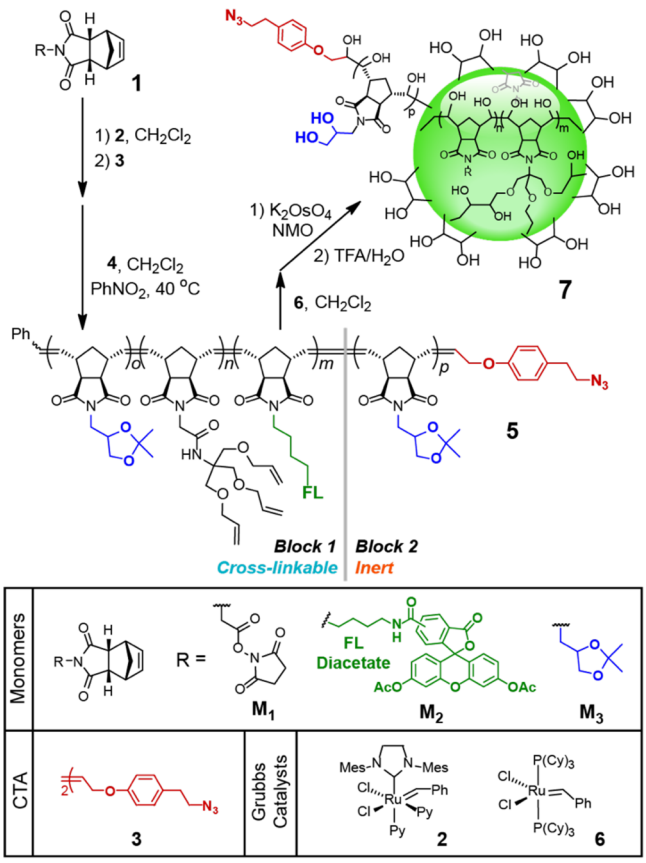

Figure 2. Scheme showing structures of the functional monomers and the detailed, ROMP-based synthesis of monovalent ONP-N_3. **2** and **6** = Grubbs catalysts (3rd and 1st generation). **4** = tris[(allyloxy)-methyl]aminomethane.

consists of two blocks: a cross-linkable block that is the precursor to the ONP framework and an inert block as a spacer, allowing accessibility of the reactive end-group. The ring-opening metathesis polymerization (ROMP) of norbornenyl derivatives **1** (structures $\mathbf{M}_{1-3}$) mediated by Grubbs catalyst **2** afforded good control over the polymer and ONP size, and allowed both block copolymer formation and the integration of one or more fluorophores (fluorescein) as reporter groups.[13] By using chain-transfer agent **3** and treating the resulting polymer with tris[(allyloxy)methyl]-aminomethane (**4**), polymer **5** with multiple side-chain alkene groups and a single reactive end-group was obtained. It was subjected to ring-closing metathesis (RCM) using Grubbs catalyst **6** and the multiple double bonds of the resultant ONP were dihydroxylated followed by deprotection of the diol and fluorescein diacetate moieties to afford water-soluble ONP **7** with a single azide group per particle. Synthetic intermediates and products were characterized by GPC and NMR (Figure S1 and S2), with data and observations consistent with the proposed structures and the previously reported results.[12b]

ONP **7** was further characterized by transmission electron microscopy (TEM). Both negatively stained and bright-field TEM images (Figure 3a and S3) showed the ONP to be

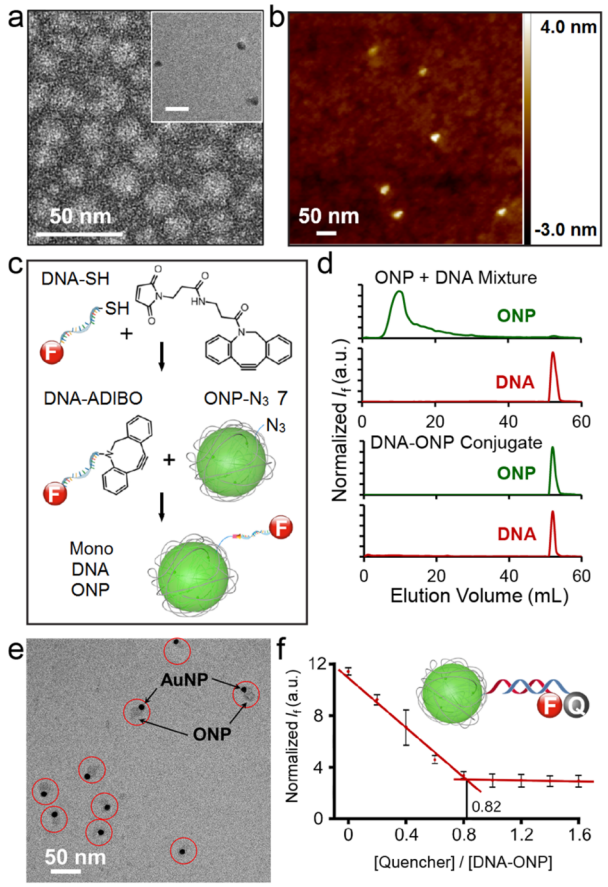

Figure 3. (a) Negatively stained and bright-field (inset) TEM images of azido-ONPs. Scale bar = 50 nm. (b) AFM images of ONPs. (c) Scheme showing the DNA-ONP conjugation chemistry. (d) Elution profiles of the mixture of DNA and ONP, and the DNA-ONP conjugate. (e) TEM images of heterodimers from monovalent DNA-ONP and 10 nm AuNP. (f) Fluorescence titration plot showing approximate 1:1 ratio of DNA to ONP in the conjugates.

roughly spherical with a diameter of ca. 15−20 nm. The ONP sizes were further confirmed by atomic force microscopy (AFM) (Figure 3b and S4). The use of the fluorescein-containing monomer $\mathbf{M}_2$ produced fluorescent ONP that could be observed both by the fluorescence spectroscopy and microscopy (Figure S5).

To conjugate DNA to the monovalent ONP in high yield, the highly efficient, strain-promoted azide−alkyne cycloaddition[14] was utilized (Figure 3c). A dual-functionalized DNA strand with 5′-AlexaFluor 594 ($Alexa_{594}$, λ_{em} = 617 nm) and 3′-thiol was used in the following studies. The DNA strand consists of an 18-base sequence designed for hybridization and a 20-base oligo-T as spacer (5′-$Alexa_{594}$-$M_{18}bT_{20}$-SH-3′).[4c] The 3′-thiolated DNA was first reacted with azadibenzocyclooctyne (ADIBO)-maleimide, giving an ADIBO-functionalized DNA oligonucleotide (Figure S6) that was then incubated with excess ONP-N_3 **7** to generate the desired 1:1 conjugate (monovalent DNA-ONP). The monovalent DNA-ONP was conveniently purified by removing unreacted ONPs with a

DOI: 10.1021/jacs.7b00065
J. Am. Chem. Soc. 2017, 139, 3623−3626

weak anion exchange column, followed by removing unreacted DNA using an Amicon centrifugal filter.

The resulting monovalent DNA-ONP conjugate showed a strong fluorescence emission at both 617 nm from $Alexa_{594}$ DNA and 522 nm from the fluorescein unit inside the ONP, (Figure S7). To demonstrate further that the DNA and ONP were covalently linked, the anion exchange elution profiles of the monovalent DNA-ONP and a simple mixture of DNA and ONP were compared (Figure 3d). The charge-free, fluorescein-loaded ONP in the mixture was first eluted by a low-salt citrate buffer and readily observed in the green channel, whereas the anionic $Alexa_{594}$ DNA oligonucleotide could only be eluted with a 2 M NaCl solution, observed in the red channel. In contrast, the monovalent DNA-ONP conjugate showed a single, coincident peak in both green and red channels when eluting with a 2 M NaCl solution. The formation and stability of the monovalent DNA-ONP conjugate was further supported by agarose gel electrophoresis (Figure S8 and S9) and confocal microscopy (Figure S10). In the agarose gel image, the monovalent DNA-ONP showed a sharper band in both green and red channels arising from emission from the fluorescein unit inside the ONP and the $Alexa_{594}$ DNA. A similar gel pattern was observed after incubating DNA-ONP with 5 mM glutathione (GSH), indicating the chemical stability of the conjugate against GSH (Figure S9). Colocalization of the two fluorescence emissions was also observed by confocal microscopy (Figure S10). Finally, ζ-potential measurements indicated the monovalent DNA-ONP to be more negatively charged (−2.6 mV) than the ONP-N_3 (1.2 mV) (Figure S11), again supporting the DNA-ONP linkage.

DNA hybridization offers an excellent orthogonal binding motif that has been useful for programming NP assembly.[15] To test whether the $M_{18}bT_{20}$-bearing monovalent DNA-ONP is indeed functional for NP assembly, it was mixed with 10 nm AuNPs conjugated with DNA strands that contain a complementary sequence to $M_{18}b$. Although the ONPs exhibit a much lower contrast than the AuNPs, heterodimers are clearly observed by TEM (Figure 3e). A more quantitative determination of the ONP/DNA ratio was carried out by fluorescence titration using a complementary DNA strand with Black Hole Quencher 2 ($M_{18}a$-BHQ2). As shown in Figure 3f, the fluorescence intensity of the $Alexa_{594}$ on the DNA-ONP conjugate decreases with increasing the molar ratio of the $M_{18}a$-BHQ2 over DNA-ONP, with the slope of the titration curve reaching a transition point. A fit of the data indicates a stoichiometric ratio of ca. 0.82, supporting the preparation of a monovalent DNA-ONP. The 18% error might be attributed to error in ONP concentration determination and the incomplete hybridization of DNA on ONP surface.

The ONP scaffold is highly porous with a MW of ca. 50 kDa and a size of ca. 15−20 nm (determined by TEM). The intrinsic porosity and large number of weakly coordinating diol and amide groups,[16] made the ONP an ideal template for the growth of functional metal NPs. Compared to a number of other nanoscale templates, the ONP allows both a scalable synthesis and a controllable, well-defined size. Thus, the chemical nature of the ONP facilitates the nucleation and growth of AuNPs within the porous scaffold upon the addition of a reducing agent. The synthesis of a monovalent AuNP and a possible mechanism is shown schematically in Figure 4a.

To study the templated synthesis process, a qualitative kinetic study was carried out by monitoring both the formation of AuNPs using their UV−vis absorption at 540 nm and the loss of the ONP using the decrease in fluorescence emission at 520 nm. Indeed, both events occurred contemporaneously (Figure 4b and S12), supporting the notion that Au deposits onto the ONP scaffold, leading to loss of the fluorescein fluorescence (Figure S13). Using ascorbic acid as the reductant afforded similar results, but with faster kinetics (Figure S14). The templated AuNPs (AuNP@ONP) using sucrose as the reducing agent showed a regular, roughly spherical morphology with an average diameter of ca. 18 nm, which compares well to the size of the ONP template used (Figure 4c and S15). The AuNP@ONP also showed stability against NaCl up to ca. 100 mM (Figure S16). Scanning transmission electron microscopy (STEM) showed a similar NP morphology and size with energy-dispersive X-ray spectroscopy (EDX) elemental mapping confirming the Au composition (Figure 4d and S17). Without the ONP template present, large Au structures (>1 μM) with irregular surfaces were formed (Figure S18).

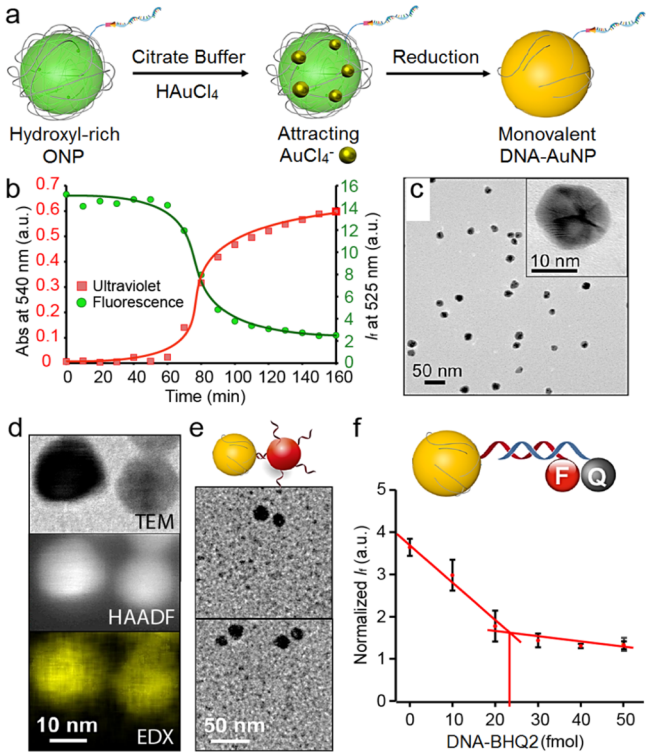

Figure 4. (a) Scheme showing a possible mechanism for the templated mono-DNA AuNP@ONP synthesis. (b) Kinetic study of the AuNP formation using UV−vis and fluorescence spectroscopy. (c) TEM images of the AuNP@ONP. (d) STEM and EDX element mapping images of AuNP@ONP. (e) Hybridization-mediated heterodimerization using the mono-DNA AuNP@ONP with commercial 10 nm AuNP functionalized with complementary DNA strands. (f) Fluorescence titration plot of mono-DNA AuNP@ONP.

The controlled metal growth process was intended to be mediated exclusively by the ONP and within the polymer scaffold, allowing the DNA to remain functional on the surface of the AuNP@ONP. The ability of the DNA strand to pair functionally was tested in several experiments using a 15−20 nm AuNP@ONP prepared according to Figure 4a. First, the presence of the DNA strand was supported by the observation of colocalization of AuNP darkfield scattering and DNA fluorescence emission (Figure S19). More importantly, DNA-directed formation of AuNP dimers was observed upon mixing the AuNP@ONP and 10 nm AuNPs conjugated with

DOI: 10.1021/jacs.7b00065
J. Am. Chem. Soc. 2017, 139, 3623−3626

complementary DNA strand in ca. 1:1 ratio (Figure 4e and S20). Finally, fluorescence titration experiments analogous to that used with the ONP (see Figure 3f) further demonstrated the functionality of the monovalent AuNP@ONP. Thus, the addition of the complementary DNA strand containing a quencher M_{18}a-BHQ2 led to a decrease in fluorescence intensity of monovalent AuNP@ONP (Figure 4f). A fit of the data suggests a transition point at ca. 23 fmol of added quencher, which correlates well with the calculated number of 18 nm AuNPs based on the overall amount of chloroauric acid added (see SI for details of the calculation), supporting the preparation of a monovalent DNA-AuNP@ONP.

Described herein is a new approach to prepare organic and AuNPs with a single functional DNA strand. The precise control over the polymer scaffold and functionality that allows independent and simultaneous control over several essential parameters, such as MW and monovalency, is generalizable and could possibly be extended to nanoparticles with other metal compositions and different sizes. Indeed, the bottom-up strategy has several advantages over conventional methods and should be applicable to even more complex functional architectures.

■ ASSOCIATED CONTENT

Supporting Information

The Supporting Information is available free of charge on the ACS Publications website at DOI: 10.1021/jacs.7b00065.

Detailed experimental procedures, NMR spectra, and additional characterization data (PDF)

■ AUTHOR INFORMATION

Corresponding Authors

*yi-lu@illinois.edu

*sczimmer@illinois.edu

ORCID

Yi Lu: 0000-0003-1221-6709

Steven C. Zimmerman: 0000-0002-5333-3437

Author Contributions

§These authors contributed equally.

Notes

The authors declare no competing financial interest.

■ ACKNOWLEDGMENTS

This work was supported by the National Science Foundation (CHE-1307404 and CTS-0120978), the Binational Science Foundation (2014116), the National Institutes of Health (MH110975).

■ REFERENCES

(1) (a) Mirkin, C. A.; Letsinger, R. L.; Mucic, R. C.; Storhoff, J. J. *Nature* **1996**, *382*, 607−609. (b) Alivisatos, A. P.; Johnsson, K. P.; Peng, X. G.; Wilson, T. E.; Loweth, C. J.; Bruchez, M. P.; Schultz, P. G. *Nature* **1996**, *382*, 609−611. (c) Aldaye, F. A.; Palmer, A. L.; Sleiman, H. F. *Science* **2008**, *321*, 1795−1799. (d) Jones, M. R.; Seeman, N. C.; Mirkin, C. A. *Science* **2015**, *347*, 840−852.

(2) (a) Park, S. Y.; Lytton-Jean, A. K. R.; Lee, B.; Weigand, S.; Schatz, G. C.; Mirkin, C. A. *Nature* **2008**, *451*, 553−556. (b) Nykypanchuk, D.; Maye, M. M.; van der Lelie, D.; Gang, O. *Nature* **2008**, *451*, 549−552. (c) Tan, S. J.; Campolongo, M. J.; Luo, D.; Cheng, W. L. *Nat. Nanotechnol.* **2011**, *6*, 268−276. (d) Kuzyk, A.; Schreiber, R.; Fan, Z. Y.; Pardatscher, G.; Roller, E. M.; Hogele, A.; Simmel, F. C.; Govorov, A. O.; Liedl, T. *Nature* **2012**, *483*, 311−314.

(3) (a) Zhao, X. J.; Tapec-Dytioco, R.; Tan, W. H. *J. Am. Chem. Soc.* **2003**, *125*, 11474−11475. (b) Liu, J. W.; Cao, Z. H.; Lu, Y. *Chem. Rev.* **2009**, *109*, 1948−1998. (c) Teller, C.; Willner, I. *Curr. Opin. Biotechnol.* **2010**, *21*, 376−391. (d) Tan, L. H.; Xing, H.; Lu, Y. *Acc. Chem. Res.* **2014**, *47*, 1881−1890.

(4) (a) Maye, M. M.; Nykypanchuk, D.; Cuisinier, M.; van der Lelie, D.; Gang, O. *Nat. Mater.* **2009**, *8*, 388−391. (b) Pinheiro, A. V.; Han, D. R.; Shih, W. M.; Yan, H. *Nat. Nanotechnol.* **2011**, *6*, 763−772. (c) Tan, L. H.; Xing, H.; Chen, H.; Lu, Y. *J. Am. Chem. Soc.* **2013**, *135*, 17675−17678. (d) Cohen-Hoshen, E.; Bryant, G. W.; Pinkas, I.; Sperling, J.; Bar-Joseph, I. *Nano Lett.* **2012**, *12*, 4260−4264.

(5) (a) Sheikholeslami, S.; Jun, Y. W.; Jain, P. K.; Alivisatos, A. P. *Nano Lett.* **2010**, *10*, 2655−2660. (b) Lim, D. K.; Jeon, K. S.; Kim, H. M.; Nam, J. M.; Suh, Y. D. *Nat. Mater.* **2010**, *9*, 60−67. (c) Tikhomirov, G.; Hoogland, S.; Lee, P. E.; Fischer, A.; Sargent, E. H.; Kelley, S. O. *Nat. Nanotechnol.* **2011**, *6*, 485−490. (d) Yan, W. J.; Xu, L. G.; Xu, C. L.; Ma, W.; Kuang, H.; Wang, L. B.; Kotov, N. A. *J. Am. Chem. Soc.* **2012**, *134*, 15114−15121.

(6) (a) Storhoff, J. J.; Elghanian, R.; Mucic, R. C.; Mirkin, C. A.; Letsinger, R. L. *J. Am. Chem. Soc.* **1998**, *120*, 1959−1964. (b) Zhang, X.; Servos, M. R.; Liu, J. *J. Am. Chem. Soc.* **2012**, *134*, 7266−7269.

(7) (a) Zanchet, D.; Micheel, C. M.; Parak, W. J.; Gerion, D.; Alivisatos, A. P. *Nano Lett.* **2001**, *1*, 32−35. (b) Claridge, S. A.; Liang, H. Y. W.; Basu, S. R.; Fréchet, J. M. J.; Alivisatos, A. P. *Nano Lett.* **2008**, *8*, 1202−1206.

(8) (a) Li, Z.; Cheng, E.; Huang, W.; Zhang, T.; Yang, Z.; Liu, D.; Tang, Z. *J. Am. Chem. Soc.* **2011**, *133*, 15284−15287. (b) Sung, K. M.; Mosley, D. W.; Peelle, B. R.; Zhang, S. G.; Jacobson, J. M. *J. Am. Chem. Soc.* **2004**, *126*, 5064−5065.

(9) (a) Sharma, J.; Chhabra, R.; Andersen, C. S.; Gothelf, K. V.; Yan, H.; Liu, Y. *J. Am. Chem. Soc.* **2008**, *130*, 7820−7821. (b) Yao, G.; Pei, H.; Li, J.; Zhao, Y.; Zhu, D.; Zhang, Y.; Lin, Y.; Huang, Q.; Fan, C. *NPG Asia Mater.* **2015**, *7*, e159. (c) Farlow, J.; Seo, D.; Broaders, K. E.; Taylor, M. J.; Gartner, Z. J.; Jun, Y. W. *Nat. Methods* **2013**, *10*, 1203−1205.

(10) (a) Sun, J. K.; Zhan, W. W.; Akita, T.; Xu, Q. *J. Am. Chem. Soc.* **2015**, *137*, 7063−7066. (b) Slocik, J. M.; Naik, R. R.; Stone, M. O.; Wright, D. W. *J. Mater. Chem.* **2005**, *15*, 749−753. (c) Suzuki, K.; Sato, S.; Fujita, M. *Nat. Chem.* **2010**, *2*, 25−29. (d) Sun, W.; Boulais, E.; Hakobyan, Y.; Wang, W. L.; Guan, A.; Bathe, M.; Yin, P. *Science* **2014**, *346*, 717−725.

(11) (a) Crooks, R. M.; Zhao, M. Q.; Sun, L.; Chechik, V.; Yeung, L. K. *Acc. Chem. Res.* **2001**, *34*, 181−190. (c) Niu, Y. H.; Yeung, L. K.; Crooks, R. M. *J. Am. Chem. Soc.* **2001**, *123*, 6840−6846. (d) Pang, X. C.; He, Y. J.; Jung, J. H.; Lin, Z. Q. *Science* **2016**, *353*, 1268−1272.

(12) (a) Bai, Y.; Xing, H.; Vincil, G. A.; Lee, J.; Henderson, E. J.; Lu, Y.; Lemcoff, N. G.; Zimmerman, S. C. *Chem. Sci.* **2014**, *5*, 2862−2868. (b) Bai, Y.; Xing, H.; Wu, P.; Feng, X.; Hwang, K.; Lee, J. M.; Phang, X. Y.; Lu, Y.; Zimmerman, S. C. *ACS Nano* **2015**, *9*, 10227−10236. (c) Harth, E.; Van Horn, B.; Lee, V. Y.; Germack, D. S.; Gonzales, C. P.; Miller, R. D.; Hawker, C. J. *J. Am. Chem. Soc.* **2002**, *124*, 8653−8660.

(13) Bielawski, C. W.; Grubbs, R. H. *Prog. Polym. Sci.* **2007**, *32*, 1−29.

(14) Agard, N. J.; Prescher, J. A.; Bertozzi, C. R. *J. Am. Chem. Soc.* **2004**, *126*, 15046−15047.

(15) (a) Xing, H.; Wang, Z.; Xu, Z.; Wong, N. Y.; Xiang, Y.; Liu, G. L.; Lu, Y. *ACS Nano* **2012**, *6*, 802−809. (b) Wong, C.-H.; Zimmerman, S. C. *Chem. Commun.* **2013**, *49*, 1679−1695.

(16) (a) Mecking, S.; Thomann, R.; Frey, H.; Sunder, A. *Macromolecules* **2000**, *33*, 3958−3960. (b) Zhou, L.; Gao, C.; Xu, W. *Langmuir* **2010**, *26*, 11217−11225. (c) Serpell, C. J.; Cookson, J.; Ozkaya, D.; Beer, P. D. *Nat. Chem.* **2011**, *3*, 478−483.

DOI: 10.1021/jacs.7b00065
J. Am. Chem. Soc. 2017, 139, 3623−3626